

## Role of State Specificity in the Temperature- and Pressure-Dependent Unimolecular Rate Constants for $\text{HO}_2 \rightarrow \text{H} + \text{O}_2$ Dissociation

Kihyung Song<sup>†</sup> and William L. Hase<sup>\*,‡</sup>

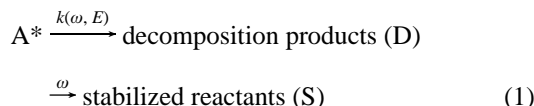
Department of Chemistry, Korea National University of Education, Chungbuk 363-791, South Korea, and  
Department of Chemistry, Wayne State University, Detroit, Michigan 48202

Received: August 7, 1997; In Final Form: November 21, 1997

Recent quantum dynamical calculations have shown that  $\text{HO}_2$  dissociates via isolated resonances, which have a distribution of rate constants that is statistical state-specific and well-described by the Porter–Thomas  $P_E(k)$  distribution. In the work presented here, this  $P_E(k)$  distribution is incorporated into RRKM theory to see how statistical fluctuations in state-specific rate constants affect the collision-averaged chemical activation rate constant  $k(\omega, E)$  and the Lindemann–Hinshelwood thermal rate constant  $k_{\text{uni}}(\omega, T)$  for  $\text{HO}_2$  dissociation. Both active and adiabatic treatments are considered for the  $K$  quantum number. The calculations suggest the effect of statistical state specificity should be detectable in measurements of  $k(\omega, E)$  and  $k_{\text{uni}}(\omega, T)$ .

### I. Introduction

The collision-averaged unimolecular dissociation of a monoenergetically excited molecule in a chemical activation experiment may be interpreted by the mechanism<sup>1</sup>



where the unimolecular rate constant is given by<sup>1</sup>

$$k(\omega, E) = \omega D/S \quad (2)$$

According to RRKM theory,<sup>2,3</sup> the dissociation of monoenergetically excited molecules is random with exponential decay, so that  $k(\omega, E)$  equals the RRKM rate constant  $k(E)$ . However, unimolecular dissociation is state-specific at the microscopic level,<sup>3–6</sup> occurring via isolated<sup>3–9</sup> or overlapping resonances<sup>10–13</sup> so that there are fluctuations<sup>14</sup> in state-specific rate constants within the energy interval  $E \rightarrow E + dE$ . As a result,  $k(\omega, E)$  in eq 1 is pressure-dependent.<sup>15,16</sup> States with large rate constants are more likely to contribute to dissociation at high pressures, while all states contribute equally in the low-pressure limit.

If the resonance states undergoing unimolecular decomposition have random wave functions, the unimolecular decomposition may be called *statistical state-specific*.<sup>3,6</sup> For this situation the resonance wave functions will be projected randomly onto any zero-order basis and the distribution of state-specific rate constants will be as statistical as possible.<sup>8</sup> If these state-specific rate constants form a continuous distribution within the energy interval  $E \rightarrow E + dE$ , it has been argued<sup>7,17</sup> that the probability of a particular  $k$  is given by the Porter–Thomas distribution<sup>18</sup>

$$P_E(k) = \Gamma\left(\frac{\nu}{2}\right)^{-1} \left(\frac{\nu}{2\bar{k}}\right) \left(\frac{\nu k}{2\bar{k}}\right)^{(\nu/2)-1} \exp\left(-\frac{\nu k}{2\bar{k}}\right) \quad (3)$$

where  $\bar{k}$  is the average state-specific rate constant

$$\bar{k} = \int_0^\infty k P(k) dk \quad (4)$$

and  $\nu$  is the “effective number of decay channels”. For large  $\nu$ ,  $P_E(k)$  approaches a delta function peaked around  $\bar{k}$ . Thus, there are no fluctuations in the state-specific rate constants and exponential decay within the energy interval  $E \rightarrow E + dE$  results, as predicted by RRKM theory.

When this  $P_E(k)$  is incorporated into the mechanism in eq 1,<sup>16</sup> it is found that  $k(\omega, E)$  has very simple forms in the high pressure  $\omega \rightarrow \infty$  and low pressure  $\omega \rightarrow 0$  limits. For the  $\omega \rightarrow \infty$  limit,  $k(\omega, E)$  is independent of  $\nu$  and equals  $\bar{k}$ . At the  $\omega \rightarrow 0$  limit,  $k(\omega, E)$  depends upon the value of  $\nu$ . It equals zero for  $\nu$  of 1 and 2, and equals  $[(\nu - 2)/\nu] \bar{k}$  for  $\nu > 2$  and finite. The latter value is the same as the value of  $k$  for the maximum in  $P(k)$  when  $\nu > 2$  and finite. Thus, the pressure dependence of  $k(\omega, E)$  becomes negligible as  $\nu$  becomes large.

The monoenergetic unimolecular rate constant  $k_{\text{uni}}(\omega, E)$  in the Lindemann–Hinshelwood mechanism for thermal unimolecular decomposition is given by<sup>16</sup>

$$k_{\text{uni}}(\omega, E) = \omega D \quad (5)$$

and is related to  $k(\omega, E)$  in eq 2 by<sup>6</sup>

$$k_{\text{uni}}(\omega, E) = \frac{\omega k(\omega, E)}{k(\omega, E) + \omega} \quad (6)$$

This relationship is valid whether or not there are fluctuations in the state-specific rate constants within the energy interval  $E \rightarrow E + dE$ . If there are fluctuations, e.g., given by  $P_E(k)$  in eq 3,  $k_{\text{uni}}(\omega, E)$  may be expressed as<sup>19</sup>

$$\bar{k}(\omega, E) = \int_0^\infty dk P_E(k) \frac{k\omega}{k + \omega} \quad (7)$$

Miller<sup>19</sup> has shown that there is a substantial differences between  $k_{\text{uni}}(\omega, E)$  curves calculated for small  $\nu$  and for  $\nu \rightarrow \infty$  which is the RRKM limit. Averaging over  $E$  gives the Lindemann–Hinshelwood thermal unimolecular rate constant<sup>6</sup>

<sup>†</sup> Korea National University of Education.

<sup>‡</sup> Wayne State University.

$$k_{\text{uni}}(\omega, T) = \frac{1}{Q} \int_0^\infty dE e^{-E/k_B T} \rho(E) k_{\text{uni}}(\omega, E) \quad (8)$$

where  $\rho(E)$  is the density of states for the reactant's active degrees of freedom and  $Q$  is the reactant's partition function.

Polik et al.<sup>8</sup> and Miller et al.<sup>20</sup> have related the Porter–Thomas  $P_E(k)$  to RRKM theory and find that  $\bar{k}$  is the RRKM rate constant  $k(E)$  and, if quantum mechanical tunneling is unimportant,  $\nu$  equals  $N^\ddagger(E)$ , the transition-state sum of states. With these prescriptions it is straightforward to use the Porter–Thomas  $P_E(k)$  and to include fluctuations in statistical state-specific rate constants when calculating  $k(\omega, E)$  and  $k_{\text{uni}}(\omega, T)$ .

In recent research Schinke and co-workers<sup>21–23</sup> performed quantum dynamical calculations for HO<sub>2</sub> dissociation, i.e.,



and showed that the wave functions for the resonance states have random characteristics. The calculated rate constants for the resonances appear to be statistical state-specific and in accord with the Porter–Thomas  $P_E(k)$  distribution.<sup>23</sup> Reaction 9 has been the focus of many previous experimental<sup>29–43</sup> and theoretical<sup>21–23,25–28,44–46</sup> studies and is a prime candidate for determining how statistical state specificity affects the unimolecular rate constants  $k(\omega, E)$  and  $k_{\text{uni}}(\omega, T)$ . This is the focus of the work presented here, which considers whether statistical state specificity can be observed in experimental measurements of collision- and energy-averaged rate constants for HO<sub>2</sub> dissociation. The DMBE IV potential energy function of Pastrana et al.,<sup>24</sup> used in previous theoretical studies<sup>21–23,25–28</sup> of HO<sub>2</sub> dissociation, is also used here.

## II. RRKM Calculations

Calculations are needed to determine the RRKM rate constant, which equals the average rate constant of the  $P_E(k)$  distribution, and  $\nu$ , which equals the transition-state sum of states. Both HO<sub>2</sub> and the dissociation transition state are treated as “almost symmetric top” rigid rotors, so that their rotational energy levels are given by<sup>47</sup>

$$E_r(J, K) = (I_a^{-1} + I_b^{-1})[J(J+1) - K^2]h^2/4 + K^2h^2/2I_c \quad (10)$$

where  $I_a \approx I_b \neq I_c$  are the moments of inertia. The quantum number  $J$  is for the total angular momentum, and  $K$  represents the projection of  $J$  onto the symmetry axis.

The quantum number  $K$  may be treated as either an *adiabatic* or *active* degree of freedom.<sup>48,49</sup> Though mixed adiabatic/active models are possible,<sup>49</sup> in this study the  $K$  quantum number is treated the same for both HO<sub>2</sub> and the transition state, i.e., either as adiabatic or active. For the adiabatic model the  $K$  quantum number is assumed to be conserved during the dissociation process, and the density of states for HO<sub>2</sub> and the sum of states for the transition state are

$$\rho(E, J, K) = \rho[E - E_r(J, K)] \quad (11)$$

$$N^\ddagger(E, J, K) = N^\ddagger[E - E_0 - E_r(J, K)] \quad (12)$$

where  $E_0$  is the unimolecular threshold. The RRKM rate constant for this model is then

$$k(E, J, K) = \frac{1}{h} \frac{N^\ddagger(E, J, K)}{\rho(E, J, K)} \quad (13)$$

For the  $K$ -active model the density and sum of states only

depend on  $E$  and  $J$  and are given by

$$\rho(E, J) = \sum_{K=-J}^J \rho(E, J, K) \quad (14)$$

$$N^\ddagger(E, J) = \sum_{K=-J}^J N^\ddagger(E, J, K) \quad (15)$$

so that the RRKM rate constant is

$$k(E, J) = \frac{1}{h} \frac{N^\ddagger(E, J)}{\rho(E, J)} \quad (16)$$

An important effect of making  $K$  active is to increase the transition-state sum of states in comparison to the  $K$ -adiabatic model.

To calculate the density of states, sum of states, and RRKM rate constants requires knowing the vibrational frequencies and principal moments of inertia for HO<sub>2</sub> and the transition state, and the unimolecular dissociation threshold  $E_0$ . The vibrational frequencies and moments of inertia for the DMBE IV potential used here are listed in Table 1 of ref 25. The threshold  $E_0$  for the DMBE IV potential is 45.45 kcal/mol.

## III. Effect of Statistical State Specificity on the HO<sub>2</sub> Collision- and Energy-Averaged Unimolecular Rate Constants

**A. Collision-Averaged Chemical Activation Rate Constant.** As discussed in the Introduction, if there are fluctuations in the state-specific rate constants within the energy interval  $E \rightarrow E + dE$ , the chemical activation rate constant  $k(\omega, E)$  in eq 2 is pressure-dependent. For statistical state specificity described by the Porter–Thomas distribution  $P_E(k)$ ,  $k(\omega, E)$  equals  $\bar{k}$  in the high-pressure limit.<sup>16</sup> In contrast, in the low-pressure limit with  $\nu > 2$  and finite, the rate constant is smaller and equals  $[(\nu - 2)/\nu] \bar{k}$ .<sup>16</sup> Here we consider the range of energy and angular momentum for which  $k(\omega, E)$  for HO<sub>2</sub> dissociation varies by 20% or more between the high- and low-pressure limits. This will occur if  $\nu \leq 10$ . Following Polik et al.<sup>8,20</sup>  $\nu$  is equated to the transition-state sum of states.

For  $J = 0$ , the sum of states  $N^\ddagger(E)$  becomes equal to 10 at  $E$  of 51.6 kcal/mol. Since  $E_0 = 45.4$  kcal/mol, there is a 6.2 kcal/mol range of energies in which the  $k(\omega, E)$  in eq 2 varies by at least 20%.

For the  $K$ -active model, with  $J > 0$ , there are two properties that affect the transition-state sum of states. First, increasing  $J$  increases the rotational energy, which decreases the energy available for vibration. This has the effect of decreasing the sum of states. However, the densities of states for all the  $K$  levels are summed with  $K$  active, which increases the sum of states. For dissociation of an almost prolate symmetric top like HO<sub>2</sub>, which of these two effects is more important depends on the value of  $J$ . For representative  $J$  values of 27, 49, 69, 98, and 120 for temperatures of 300, 1000, 2000, 4000, and 6000 K, respectively,<sup>50</sup>  $\nu = N^\ddagger(E, J)$  becomes equal to 11 [i.e., due to symmetry for  $K$  and  $-K$ , there is no 10 for  $N^\ddagger(E, J)$ ] at  $E - E_0$  of 0.73, 2.16, 4.15, 8.21, and 12.2 kcal/mol. Thus, increasing  $J$  from zero first decreases and then increases the range of energy for which there is a substantial change in  $k(\omega, E)$  between the high- and low-pressure limits.

To obtain a value for  $\nu = N^\ddagger(E, J, K)$  of 10 when  $K$  equals  $J$  for the  $K$ -adiabatic model, much higher values of energy are required than those given above for the  $K$ -active model. For  $K$

$= J$  of 27, 49, 69, 98, and 120,  $\nu$  becomes equal to 10 at the respective energies  $E - E_0$  of 9.8, 18.1, 29.8, 53.7, and 77.4 kcal/mol. If  $J$  is maintained at this value, but representative values of  $K$  are chosen for the temperatures of 300, 1000, 2000, 4000, and 6000 K,<sup>51</sup> which are 19, 35, 49, 69, and 85, respectively, the energies  $E - E_0$  at which  $N^\ddagger(E, J, K)$  equals 10 are lower and are, respectively, 8.3, 13.3, 20.1, 33.8, and 47.9 kcal/mol. The energies are even lower and equal 6.8, 8.2, 10.2, 14.3, and 18.3, respectively, for the same set of temperatures if  $K$  equals zero.

The above examples illustrate that, regardless of whether the  $K$ -active or  $K$ -adiabatic model is appropriate for HO<sub>2</sub> decomposition, there is a broad range of energy and angular momentum for which statistical state specificity should be experimentally detectable in the monoenergetic pressure-dependent chemical activation rate constant  $k(\omega, E)$ . As discussed previously,<sup>15</sup>  $k(\omega, E)$  is much less sensitive to  $P_E(k)$  than are other kinetic properties such as the time-dependent population of monoenergetically excited molecules in the absence of collisions. However, with careful experiments it should be possible to measure changes in  $k(\omega, E)$  versus pressure as a result of the fluctuations in  $P_E(k)$ .

**B. Pressure- and Temperature-Dependent Lindemann–Hinshelwood Thermal Rate Constant.** It is also of interest to determine the sensitivity of the Lindemann–Hinshelwood rate constant  $k_{\text{uni}}(\omega, T)$  in eq 8 to statistical state specificity for HO<sub>2</sub> dissociation. To calculate  $k_{\text{uni}}(\omega, T)$  it is useful to write  $k_{\text{uni}}(\omega, E)$  in eq 7 as<sup>19</sup>

$$\frac{k_{\text{uni}}(\omega, E)}{\bar{k}} = \Gamma\left(\frac{\nu}{2}\right)^{-1} \int_0^\infty dz \left(\frac{z\nu}{2}\right)^{\nu/2} \exp\left(-\frac{z\nu}{2}\right) \frac{\lambda}{\lambda + z} \\ = \frac{2}{\nu} \int_0^\infty dx e^{-x} \exp\left[\frac{\nu}{2} \ln x - \ln \Gamma\left(\frac{\nu}{2}\right)\right] \frac{\lambda}{\lambda + \frac{2x}{\nu}} \quad (17)$$

where  $x = z\nu/2$ ,  $z = k/\bar{k}$ ,  $\lambda = \omega/\bar{k}$ , and  $\bar{k}$  is the average rate constant for the Porter–Thomas distribution  $P_E(k)$ . The exponential and logarithmic functions in the lower line of eq 17 were used to prevent overflow errors when  $\nu$  gets large.

The notation in eq 17 is incomplete in that it does not explicitly include angular momentum. For the  $K$ -active model,  $k_{\text{uni}}(\omega, E)$  becomes  $k_{\text{uni}}(\omega, E, J)$ ,  $\bar{k}$  is the RRKM rate constant  $k(E, J)$  in eq 16,  $\nu$  equals  $N^\ddagger(E, J)$  in eq 15, and  $k_{\text{uni}}(\omega, E, J)/\bar{k}$  in eq 17 may be expressed as  $I_{P-T}(\omega, E, J)$ , the Porter–Thomas integral over  $k$ . The thermal rate constant  $k_{\text{uni}}(\omega, T)$  may then be written as

$$k_{\text{uni}}(\omega, T) = \frac{1}{Q} \int_0^\infty dE e^{-E/kT} \sum_{J=0}^{J_{\text{max}}(E)} (2J+1) I_{P-T}(\omega, E, J) N^\ddagger(E, J) \quad (18)$$

For the  $K$ -adiabatic model,  $k_{\text{uni}}(\omega, E)$  in eq 17 becomes  $k_{\text{uni}}(\omega, E, J, K)$ ,  $\bar{k}$  is the RRKM rate constant  $k(E, J, K)$  in eq 13,  $\nu$  equals  $N^\ddagger(E, J, K)$  in eq 12, and  $k_{\text{uni}}(\omega, E, J, K)/\bar{k}$  may be expressed as  $I_{P-T}(\omega, E, J, K)$ . The rate constant  $k_{\text{uni}}(\omega, T)$  for the  $K$ -adiabatic model may then be expressed as

$$k_{\text{uni}}(\omega, T) = \frac{1}{Q} \int_0^\infty dE e^{-E/kT} \sum_{J=0}^{J_{\text{max}}(E)} (2J+1) \times \\ \sum_{K=-J}^J I_{P-T}(\omega, E, J, K) N^\ddagger(E, J, K) \quad (19)$$

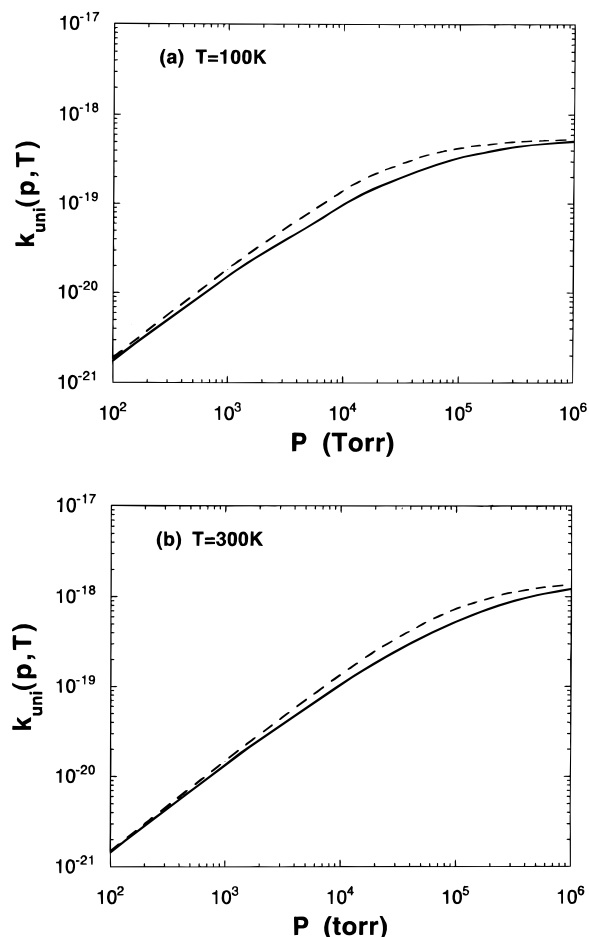


**Figure 1.**  $k_{\text{uni}}(\omega, T)$  curves at (a) 100 K and (b) 300 K with  $J = 0$ : (---), standard RRKM theory; (—), RRKM theory with the Porter–Thomas  $P_E(k)$  distribution. Including a Porter–Thomas distribution of rate constants affects  $k_{\text{uni}}(\omega, T)$  at intermediate pressures. See text for discussion.

Equations 18 and 19 were used to calculate  $k_{\text{uni}}(\omega, T)$  for the  $K$ -active and  $K$ -adiabatic models. The collision frequency  $\omega$  is calculated using the same procedure described in ref 25.

The first set of calculations is for  $J = 0$  and involves a comparison of  $k_{\text{uni}}(\omega, T)$  calculated with (1) the standard RRKM protocol with exponential decay for each energy interval  $E \rightarrow E + dE$  and (2) the Porter–Thomas distribution of state-specific rate constants within the energy interval  $E \rightarrow E + dE$ . The difference between the two sets of rate constants decreases as the temperature is increased, and results for  $T$  of 100 and 300 K are plotted in Figure 1. The maximum difference between the two curves is 31% at 100 K and  $1 \times 10^4$  Torr and 29% at 300 K and  $5 \times 10^4$  Torr. These plots also show that including a distribution of state-specific rate constants only affects  $k_{\text{uni}}(\omega, T)$  at intermediate pressures. Equations 6–8 show that this result is expected. In the second-order low-pressure limit,  $k_{\text{uni}}(\omega, T)$  is proportional to  $\omega$  and the Boltzmann-averaged density of states of reacting molecule.<sup>2</sup> At high pressures it is only the average rate constant  $\bar{k}$  for each energy interval which contributes to  $k_{\text{uni}}(\omega, T)$ .<sup>19</sup>

The difference between the standard RRKM  $k_{\text{uni}}(\omega, T)$  curve and the one which includes the effect of  $P_E(k)$  increases as the temperature is decreased because reaction at low energies make more important contributions to the rate at low temperatures. As the energy decreases, the average rate constants  $\bar{k}$ , given by RRKM theory, decrease since the transition-state sums of states become smaller. This sum of states equals  $\nu$ , which determines

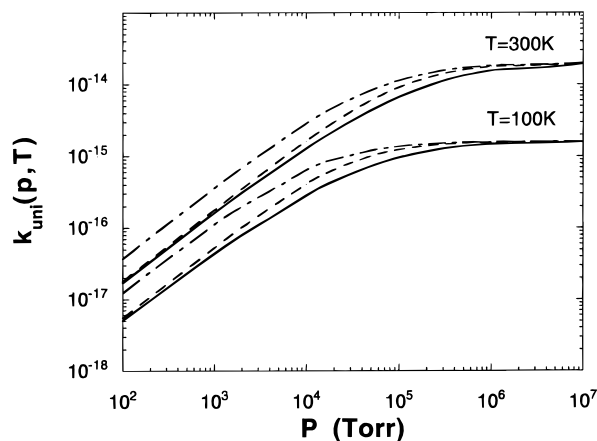


**Figure 2.** Same as Figure 1, except that a thermal distribution is included for  $J$  and both  $K$ -active and  $K$ -adiabatic models are considered. For the  $K$ -active model (---) there is only a small difference between the standard RRKM calculation and the one with the  $P_E(k)$  distribution. For the  $K$ -adiabatic model, a difference is observed between (---) standard RRKM and (—) RRKM with the  $P_E(k)$  distribution. See text for discussion.

the width of the  $P_E(k)$  distribution. Thus, the  $P_E(k)$  distributions contributing to  $k_{\text{uni}}(\omega, T)$  broaden as the temperature is lowered and the difference with standard RRKM increases. At a high temperature of 6000 K there is no detectable difference between the standard RRKM  $k_{\text{uni}}(\omega, T)$  curve and the one calculated with the  $P_E(k)$  distribution.

Plots of the  $k_{\text{uni}}(\omega, T)$  curves calculated at 100 and 300 K with the active and adiabatic treatments of  $K$  are given in Figure 2. The differences between the standard RRKM  $k_{\text{uni}}(\omega, T)$  curve and the one which includes the  $P_E(k)$  distribution is much smaller for the  $K$ -active model than for the  $K$ -adiabatic model. This is because the transition-state sum of states and, thus,  $\nu$  are much larger for the  $K$ -active model. The  $K$ -adiabatic model and the  $J = 0$  calculations, shown in Figure 1, give similar differences between the  $k_{\text{uni}}(\omega, T)$  curves determined from standard RRKM theory and that with  $P_E(k)$  included.

At the high-pressure limit the  $K$ -active and  $K$ -adiabatic models give the same unimolecular rate constant, as discussed previously.<sup>49</sup> This arises from the use of nonvariational transition state in this study. However, in the low-pressure limit the two models give different rate constants, since the rate becomes directly proportional to the number of reactive states of the molecule which can evolve to the states at the transition state.<sup>49</sup> This number of states is much smaller for the adiabatic model. The  $K$ -adiabatic model gives a rate constant which is 2.3 and 2.1 times smaller, respectively, at 100 and 300 K.

The different theoretical models give similar  $k_{\text{uni}}(\omega, T)$  curves as the temperature is increased. This is shown in Figure 3, where the maximum percent difference ( $[k(\text{bigger}) - k(\text{smaller})]/k(\text{bigger}) \times 100$ ) between two  $k_{\text{uni}}(\omega, T)$  curves is plotted versus temperature. A comparison is made between the standard RRKM and RRKM with  $P_E(k)$  curves for the  $K$ -adiabatic model, the same comparison is made for the  $K$ -active model, and the RRKM with  $P_E(k)$  curves are compared for the  $K$ -active and  $K$ -adiabatic models. The maximum difference between the latter two curves occurs in the low-pressure limit and varies from a factor of 2.3 at 100 K to near agreement at 4000 K. The maximum difference between the standard RRKM and RRKM with  $P_E(k)$  curves for the  $K$ -adiabatic model and for the  $K$ -active model occurs at a different pressure as the temperature is changed. For example, for the  $K$ -adiabatic model the maximum difference between the two curves smoothly increases from a

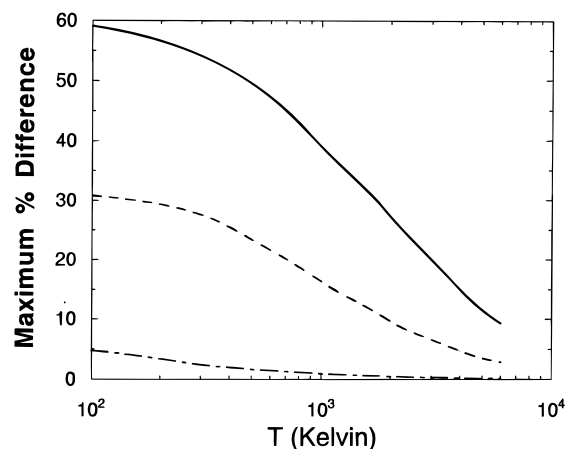


**Figure 3.** Maximum percent difference between two  $k_{\text{uni}}(\omega, T)$  curves: (---), standard RRKM and RRKM with  $P_E(k)$  curves for the  $K$ -active model; (---), standard RRKM and RRKM with  $P_E(k)$  curves for the  $K$ -adiabatic model; (—), RRKM with  $P_E(k)$  curves for the  $K$ -adiabatic and  $K$ -active models.

pressure of  $1 \times 10^4$  to  $1 \times 10^6$  Torr as the temperature is increased from 100 to 6000 K. The difference between the standard RRKM and RRKM with  $P_E(k)$  curves is much smaller for the  $K$ -adiabatic model for reasons stated above.

#### IV. Summary

Recent quantum dynamical calculations have shown that  $\text{HO}_2$  decomposes via isolated resonances that have wave functions with random attributes, indicative of chaos.<sup>21–23,27</sup> This work has suggested that at the microscopic level the unimolecular dissociation of  $\text{HO}_2$  is statistical state-specific,<sup>6</sup> with fluctuations in the resonance rate constants well-described by the Porter–Thomas<sup>18</sup>  $P_E(k)$  distribution. In the work presented here this  $P_E(k)$  distribution has been incorporated into standard RRKM theory to determine how random fluctuations in the  $\text{HO}_2 \rightarrow \text{H} + \text{O}_2$  state-specific rate constants affect the  $\text{HO}_2$  collision-averaged chemical activation rate constant  $k(\omega, E)$  and the Lindemann–Hinshelwood thermal unimolecular rate constant  $k_{\text{uni}}(\omega, T)$ . Both active and adiabatic models are used to describe the  $K$  quantum number for  $\text{HO}_2$  and the transition state. There is considerable interest in determining which of these models is more appropriate for unimolecular reactions.<sup>52,53</sup> The following are the major findings of this study.

(1) Including the  $P_E(k)$  distribution causes  $k(\omega, E)$  to decrease from the RRKM value at high pressure to  $(\nu - 2)/\nu$  times the RRKM rate constant at low pressure. The term  $\nu$  is the effective number of decay channels and is equated to the sum of states at the transition state. There is a broad range of energies and angular momentum for which the pressure dependence of  $k(\omega, E)$  should be measurable.

(2) Including  $P_E(k)$  only affects  $k_{\text{uni}}(\omega, T)$  at intermediate pressure, since it does not affect  $k_{\text{uni}}(\omega, T)$  in either the low- or high-pressure limit. The effect of  $P_E(k)$  increases as the temperature is decreased, since the width of the  $P_E(k)$  contributing to  $k_{\text{uni}}(\omega, T)$  increases as the temperature is decreased. The effect of  $P_E(k)$  should be detectable in  $k_{\text{uni}}(\omega, T)$  curves measured at low temperatures. One way to probe for fluctuations in the underlying state specific rate constants from a measurement of  $k_{\text{uni}}(\omega, T)$  is to compare the experimental  $k_{\text{uni}}(\omega, T)$  with the prediction of standard RRKM theory. If there are fluctuations, the difference between experiment and standard RRKM theory will increase with decrease in temperature.

(3) In the low-pressure limit there is an appreciable difference between the  $k_{\text{uni}}(\omega, T)$  curves calculated with the active and

adiabatic models for the  $K$  quantum number. This difference decreases as the temperature increases. For example, at 100 K, the  $k_{\text{uni}}(\omega, T)$  with  $K$ -active is 2.3 times larger, while it is only 11% larger at 4000 K.

**Acknowledgment.** This research was supported by the National Science Foundation. The authors thank Reinhard Schinke and Abigail Dobbyn for helpful discussions and Ronald J. Duchovic for providing his versions of the KAPPA and UNIMOL programs. K.S. thanks the Korea National University of Education for allowing a summer visit to Wayne State University in 1996 to perform this research.

## References and Notes

- (1) Rabinovitch, B. S.; Setser, D. W. *Adv. Photochem.* **1964**, *3*, 1.
- (2) Gilbert, R. G.; Smith, S. C. *Theory of Unimolecular and Recombination Reactions*; Blackwell Scientific: Oxford, 1990.
- (3) Baer, T.; Hase, W. L. *Unimolecular Reaction Dynamics. Theory and Experiments*; Oxford University Press: New York, 1996.
- (4) Mies, F. H.; Krauss, M. *J. Chem. Phys.* **1966**, *45*, 4455.
- (5) Mies, F. H. *J. Chem. Phys.* **1969**, *51*, 798.
- (6) Hase, W. L.; Cho, S.-W.; Lu, D.-h.; Swamy, K. N. *Chem. Phys.* **1989**, *139*, 1.
- (7) Polik, W. F.; Moore, C. B.; Miller, W. H. *J. Chem. Phys.* **1988**, *89*, 3584.
- (8) Polik, W. F.; Guyer, D. R.; Miller, W. H.; Moore, C. B. *J. Chem. Phys.* **1990**, *92*, 3471.
- (9) Wagner, A. F.; Bowman, J. M. *J. Phys. Chem.* **1987**, *91*, 5314.
- (10) Someda, K.; Nakamura, H.; Mies, F. H. *Chem. Phys.* **1994**, *187*, 195.
- (11) Someda, K.; Nakamura, H.; Mies, F. H. *Prog. Theor. Phys. Suppl.* **1994**, *116*, 443.
- (12) Peskin, U.; Reisler, H.; Miller, W. H. *J. Chem. Phys.* **1994**, *101*, 9672.
- (13) Peskin, U.; Miller, W. H.; Reisler, H. *J. Chem. Phys.* **1995**, *102*, 8874.
- (14) Levine, R. D. *Adv. Chem. Phys.* **1987**, *70*, 53.
- (15) Lu, D.-h.; Hase, W. L. *J. Chem. Phys.* **1989**, *90*, 1557.
- (16) Lu, D.-h.; Hase, W. L. *J. Phys. Chem.* **1989**, *93*, 1681.
- (17) Levine, R. D. *Ber. Bunsen-Ges. Phys. Chem.* **1988**, *92*, 222.
- (18) Porter, C. E.; Thomas, R. G. *Phys. Rev.* **1956**, *104*, 483.
- (19) Miller, W. H. *J. Phys. Chem.* **1988**, *92*, 4261.
- (20) Miller, W. H.; Hernandez, R.; Moore, C. B.; Polik, W. F. *J. Chem. Phys.* **1990**, *93*, 5657.
- (21) Dobbyn, A. J.; Stumpf, M.; Keller, H.-M.; Schinke, R. *J. Chem. Phys.* **1995**, *103*, 9947.
- (22) Dobbyn, A. J.; Stumpf, M.; Keller, H.-M.; Hase, W. L.; Schinke, R. *J. Chem. Phys.* **1995**, *102*, 5867.
- (23) Dobbyn, A. J.; Stumpf, M.; Keller, H.-M.; Schinke, R. *J. Chem. Phys.* **1996**, *104*, 8357.
- (24) Pastrana, M. R.; Quintales, L. A. M.; Brandão, J.; Varandas, A. J. C. *J. Phys. Chem.* **1990**, *94*, 8073.
- (25) Duchovic, R. J.; Pettigrew, J. D. *J. Phys. Chem.* **1994**, *98*, 10974.
- (26) Song, K.; Peslherbe, G. H.; Hase, W. L.; Dobbyn, A. J.; Stumpf, M.; Schinke, R. *J. Chem. Phys.* **1995**, *103*, 8891.
- (27) Stumpf, M.; Dobbyn, A. J.; Mordaunt, D. H.; Keller, H.-M.; Fluethmann, H.; Schinke, R. *Faraday Discuss.* **1995**, *102*, 193.
- (28) Yang, C.-Y.; Klippenstein, S. J. *J. Chem. Phys.* **1995**, *103*, 7287.
- (29) Miller, J. A.; Kee, R. J.; Westbrook, C. K. *Annu. Rev. Phys. Chem.* **1990**, *41*, 345.
- (30) Nelson, D. D.; Zahniser, M. S. *J. Mol. Spectrosc.* **1991**, *150*, 527.
- (31) Adhikari, N.; Hamilton, I. *J. Phys. Chem.* **1991**, *95*, 6470.
- (32) Burkholder, J. B.; Hammer, P. D.; Howard, C. J.; Towle, J. P.; Brown, J. M. *J. Mol. Spectrosc.* **1992**, *151*, 493.
- (33) Fisher, E. R.; Armentrout, P. B. *J. Phys. Chem.* **1990**, *94*, 4396.
- (34) Holmes, J. L.; Lossing, F. P.; Mayer, P. M. *J. Am. Chem. Soc.* **1991**, *113*, 9723.
- (35) Masten, D. A.; Hanson, R. K.; Bowman, C. T. *J. Phys. Chem.* **1990**, *94*, 7119.
- (36) Yuan, T.; Wang, C.; Yu, C.-L.; Frenklach, M.; Rabinowitz, M. J. *J. Phys. Chem.* **1991**, *95*, 1258.
- (37) Rubahn, H.-G.; van der Zinde, W. J.; Zhang, R.; Bronikowski, M. J.; Zare, R. N. *Chem. Phys. Lett.* **1991**, *186*, 154.
- (38) Shin, K. S.; Michael, J. V. *J. Chem. Phys.* **1992**, *95*, 262.
- (39) Du, H.; Hessler, J. P. *J. Chem. Phys.* **1992**, *96*, 1077.
- (40) Hughes, K. J.; Lightfoot, P. D.; Pilling, M. J. *Chem. Phys. Lett.* **1992**, *191*, 581.
- (41) Carleton, K. L.; Kessler, W. J.; Marinelli, W. J. *J. Phys. Chem.* **1993**, *97*, 6412.
- (42) Yu, C.-L.; Frenklach, M.; Masten, D. A.; Hanson, R. K.; Bowman, C. T. *J. Phys. Chem.* **1994**, *98*, 4770.
- (43) Michael, J. V. *Prog. Energy Combust. Sci.* **1992**, *18*, 327.
- (44) Song, K.; Chesnavich, W. J. *J. Chem. Phys.* **1989**, *91*, 4664.
- (45) Song, K.; Chesnavich, W. J. *J. Chem. Phys.* **1990**, *93*, 5751.
- (46) Lemon, W. J.; Hase, W. L. *J. Phys. Chem.* **1987**, *91*, 1596.
- (47) Townes, C. H.; Schalow, A. L. *Microwave Spectroscopy*; McGraw-Hill: New York, 1955; pp 84–86.
- (48) Zhu, L.; Hase, W. L. *Chem. Phys. Lett.* **1990**, *175*, 117.
- (49) Zhu, L.; Chen, W.; Hase, W. L.; Kaiser, E. W. *J. Phys. Chem.* **1993**, *97*, 311.
- (50) The  $J$  values were calculated from the relationship  $J = (2IRT)^{1/2}/h$ , where  $I$  is the average of  $I_a$  and  $I_b$ ; see eq 10.
- (51) The  $K$  values were calculated from the relationship  $K = (I_c RT)^{1/2}/h$ ; see eq 10.
- (52) North, S. W.; Hall, G. E. *J. Chem. Phys.* **1997**, *106*, 60.
- (53) North, S. W.; Hall, G. E. *Ber. Bunsen-Ges. Phys. Chem.* **1997**, *101*, 459.